Int. J. Electrochem. Sci., 14 **(2019)** 3535 – 3552, doi: 10.20964/2019.04.40

International Journal of
ELECTROCHEMICAL
SCIENCE
www.electrochemsci.org

Structural and Optical Properties of Co_3O_4 Nanoparticles Prepared by Sol-gel Technique for Photocatalytic Application

A.B. Vennela[1], *D. Mangalaraj*[2,*], *N. Muthukumarasamy*[1], *S. Agilan*[1], *K.V. Hemalatha*[3,*]

[1] Department of Physics, Coimbatore Institute of Technology, Coimbatore-641014, India.
[2]Department of Nanoscience and Technology,Bharathiar University, Coimbatore- 641046, India.
[3] Department of Chemistry, Coimbatore Institute of Technology, Coimbatore-641014, India.
[*]E-mail: mangalaraj@buc.edu.in, hemalatha.kv@cit.edu.in

Received: 16 October 2018 / *Accepted:* 11 February 2019 / *Published:* 10 March 2019

Co_3O_4 (Cobalt Oxide) nanoparticles (NPs) were synthesized via sol-gel method by taking cobalt acetate (Co(OAC)) as a precursor material at four different concentrations like 0.06, 0.07, 0.08,and 0.09 M. The obtained Co_3O_4 was used as the photocatalyst for the degradation of methylene blue dye. The phase pure cubic spinel cobalt oxide formation was confirmed by powder X-ray diffraction (PXRD). The surface morphology and elemental analysis were studied by FESEM and EDAX. The SEM image showed that the particle size ranged from 200 nm to 1μm with respect to the concentration of the cobalt acetate precursor. Surface defects, vibrational and rotational modes of Co_3O_4 was determined by Raman studies. The functional groups of the cubic spinel Co_3O_4 were determined by the Fourier Transform Infrared Spectroscopic (FTIR) analysis. The optical behavior of the prepared material was investigated by UV-Vis and PL spectroscopic studies. The band gap of Co_3O_4 varied as1.29 eV and 3.34 eV for Co_3O_4-006, 1.39 eV and 3.53 eV for Co_3O_4-007, 1.59 eV and 3.58 eV for Co_3O_4-008 and 1.63 eV and 3.65 eV for Co_3O_4-009 is due to the quantum confinement effect. The Co_3O_4-006 showed 93.8% degradation of methylene blue dye under visible light irradiation.

Keywords: Co_3O_4 Nanoparticle, Sol-gel method, Structural, Optical property, Photocatalytic activity

1. INTRODUCTION

In the last few decades the rapid development of textile, leather, paper, food and cosmetics industries have produced a large number of active dyes [1,2]. These dyes are non-biodegradable, highly toxic in water and act as a serious threat to the ecosystem [3].Therefore, many efforts have been taken by the researchers for the removal of organic pollutants before it enters into the living environment through various methods such as biodegradation [4], chemical degradation [5] and physical degradation [6]. Among them, photocatalytic degradation has attracted much attention because of the advantages like low cost, easily controlled operation, non-selective oxidation, and so on. Various semiconductor photocatalyst like TiO_2, WO_3, Ta_2O_5, ZnS and CdS etc., were used as a potential candidate for photocatalytic degradation of organic textile dyes in effluent treatments [2]. Cobalt oxide (Co_3O_4) nanoparticle, a p-type semiconductor has drawn increased attention in recent years for the photodegradation of dye pollutants due to its high surface-to-volume ratio, low cost, environment-friendly, easy preparation, excellent chemical and physical stability [3]. Also, Co_3O_4 nanomaterial possesses outstanding optical, electrical and magnetic [7] properties that was used for various applications like gas sensors [8-10], supercapacitors [11], lithium ion batteries [12-15], CO oxidation at low temperature [16-18] and energy storage [19, 20] devices.

The behavior of the nanoparticle depends on the structural morphology, surface area, porosity and so on. The nanoparticle can be prepared by various techniques like sol gel, hydrothermal, flame pyrolysis and chemical reduction. The structural morphology varies with respect to the methodology adopted. Zhao et al. 2013 has developed nanowire, nanorod and spherical shaped Co_3O_4 nanostructures using hydrothermal method for degradation of methyl orange dye under UV light irradiation. The prepared spherical shaped Co_3O_4 nanostructures showed good photocatalytic activity than the nanowire and nanorod Co_3O_4 nanostructures with 81% degradation efficiency [21]. Warang et al. 2012 has reported Co_3O_4 nanoparticles prepared by pulsed laser deposition method and so grown photocatalyst acted as a potential photocatalyst in methylene blue dye degradation under UV light radiation [22]. Chen et al. 2009 developed Co_3O_4 hollow microspheres through two-step process for methyl orange dye degradation under UV light irradiation [23].

The present study is focused to develop Co_3O_4 nanoparticles through polymer-assisted sol-gel technique as it is considered to be the most efficient affordable method in producing controlled nanostructure materials. Polymer such as polyamide, polyimide, polyvinyl alcohol, collagen, polystyrene, chitosan, polypropylene, polycaprolactone and elastin based materials were recently used in the preparation of nanomaterials. Polyvinylpyrrolidone was used in the present study (PVP) because it influences in surface functionalization and size variations [24-29]. The main objective of the present investigation is to monitor the influence of the different concentrations of cobalt acetate precursor on structural morphology and influence of cobalt oxide as photocatalyst on the degradation of methylene blue dye. The prepared cobalt oxide nanomaterial was characterized to assess its structural morphology, optical property and photodegradation efficiency.

2. EXPERIMENTAL

2.1. Materials required

Cobalt acetate, Polyvinylpyrrolidone (PVP), and Triethanol amine were used as precursor. Methylene blue (Merck, India) dye was used as the model pollutant.

2.2 Preparation of cobalt oxide nanoparticles

The procedure of the preparation of cobalt oxide (Co_3O_4) material as follows. About 2.5 gm of Polyvinylpyrrolidone (PVP) was mixed with 5 mL of distilled water to form a homogeneous solution and kept aside. Subsequently, 0.06 M of cobalt acetate was mixed with 10 mL of deionized water and vigorously stirred for half an hour. The homogeneous PVP solution was added dropwise into cobalt acetate solution to form a pink colored mixture. Triethanol amine of 3 mL was slowly dropped to the mixture, and kept on stirring another 30 minutes until a homogeneous transparent solution was obtained. The obtained solution was heated to 300 °C for 2 hours and the resultant powder was annealed at 450 °C for 3 hours. The analogous preparation was carried out by varying the concentration of cobalt acetate (Co(OAC) as 0.07 M, 0.08 M and 0.09 M. The cobalt oxide prepared from 0.06 M, 0.07 M, 0.08 M and 0.09 M of cobalt acetate was abbreviated as (Co_3O_4-006), (Co_3O_4-007), (Co_3O_4-008) and (Co_3O_4-009), respectively. After annealing, the sample was cooled, ground and characterized for XRD, FT-IR, RAMAN, FESEM, EDAX, TEM, UV-Vis spectroscopy, PL, and photocatalytic degradation activity. The cobalt oxide material was characterized by X-Ray Diffraction technique using Rigaku - XRD, Ultima-IV X-Ray diffraction (1.5432 Å) for phase identification and structural confirmation. The functional group of the materials was recorded by Alpha ECO ATR (Bruker) at the spectral range of 4000 to 500 cm^{-1}. To analyze the molecular vibrations and crystal structures Raman Analyzer -EZ Raman C1S, Make: TSI, Laser Wavelength:532 nm was used. The structural morphology was analyzed from FESEM∑ Version -Carl Zeiss, Germany, 5.07 Beta and the elemental compositions were studied by using EDAX.HRTEM (FeiTecnai G220 Twin- 200 KV) analysis. Ultraviolet-visible (UV–vis) spectroscopic analysis was carried out by Optizen – 3220 UV, MECASYS. The photoluminescence was measured using Cary Eclipse - G9800AA. The photocatalytic work was carried out using Pyrex reactor with 400 W mercury lamp and the concentration of the dye was carried out by Optizen – 3220 UV, MECASYS.

2.3. Photocatalytic degradation study

The performance of Co_3O_4photocatalyst on degradation of methylene blue dye was carried out with Pyrex reactor. About 0.1 gm of prepared Co_3O_4photocatalyst was added with 50 mL of 10 ppm aqueous methylene blue dye solution. The dye and the photocatalyst was exposed to 400 W Philips, mercury lamp under stirring. The reaction was under dark condition to achieve the adsorption-desorption equilibrium for about 30 minutes. After 30 minutes the reaction mixture was exposed to visible light irradiation. The samples were collected to monitor the extent of degradation at regular time interval (15 min), centrifuged and analyzed using UV-Visible spectrophotometer at wavelength (λ_{max}) 664 nm. The percentage of dye degraded has been calculated using equation (1).

$$\text{Percentage of degradation} = \left(\frac{C_o - C_t}{C_0}\right)\times 100 \quad \cdots\cdots\cdots\cdots\cdots\blacktriangleright \quad (1)$$

where C_o is the initial concentration of the dye solution and C_t is the final concentration of the dye solution at time t. Photocatalytic kinetics was carried out using Langmuir-Hinshelwood (L-H) kinetic model using equation (2);

$$\ln\left(\frac{C_t}{C_o}\right) = k_{app}t \quad \cdots\cdots\cdots\cdots\cdots\cdots\cdots\blacktriangleright \quad (2)$$

Where k_{app} is the apparent reaction rate constant of pseudo first order reaction and t is the time required for reaction.

3. RESULT AND DISCUSSION

3.1 X-ray diffraction (XRD) studies

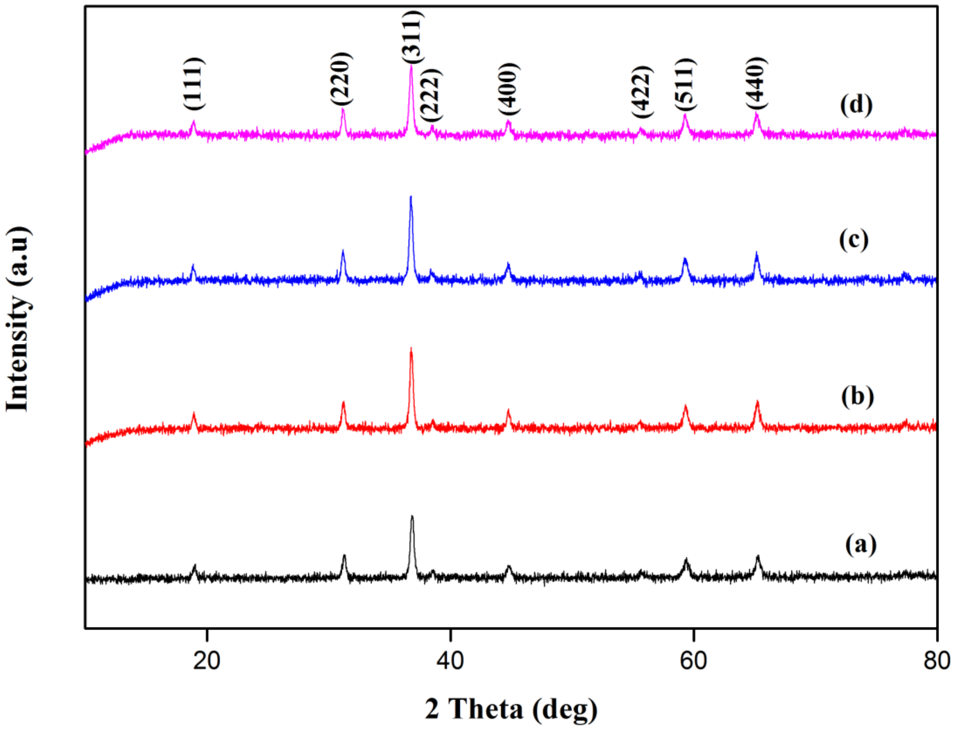

Figure 1. XRD pattern of cobalt oxide nanoparticles prepared from different concentration of cobalt acetate annealed at 450°C by sol-gel method. (a) Co_3O_4-006, (b) Co_3O_4-007, (c) Co_3O_4-008 and (d) Co_3O_4-009

Figure 1, showed the XRD pattern of Co_3O_4-006, Co_3O_4-007, Co_3O_4-008 and Co_3O_4-009. TheCo_3O_4 showed a sharp narrow peak with the diffraction pattern of (111), (220), (311), (222), (400), (422), (511) and (440) at 2θ angle of 18.9, 31.14, 36.68, 38.51, 44.68, 55.75, 59.31 and 65.10 is the indication of the crystalline nature of the material with face-centered cubic spinel structure of Fd3m space group. The absence of diffraction peaks related to CoO and other phases confirm the formation of phase pure Co_3O_4 which is coherent with the standard JCPDS No: 76-1802 [28]. The average crystallite size was calculated using Debye-Scherrer's equation (3)

$$D=\frac{0.9\lambda}{\beta\cos\theta} \quad \cdots\cdots\cdots\cdots\blacktriangleright \quad (3)$$

where λ is the wavelength of Cu-kα radiation, β is the full width half-maximum (FWHM) in radians, and θ is the angle of diffraction (in radians). The average crystallite size of Co_3O_4-006, Co_3O_4-007, Co_3O_4-008 and Co_3O_4-009 was found to be 26.22 nm, 26.50 nm, 29.85 nm and 30.23 nm respectively. The crystallite size increases with increase in the concentration of the Co(OAC) precursor. The lattice constant "a" calculated from the hkl value of 311 peak was found to be 8.087 Å, 8.104 Å, 8.108Å, and 8.104Å for Co_3O_4-006, Co_3O_4-007, Co_3O_4-008 and Co_3O_4-009 respectively. From the calculated crystallite size, dislocation density (δ) was estimated by the following relation (4);

$$\delta = \frac{1}{D^2} \quad \cdots\cdots\cdots\cdots\blacktriangleright \quad (4)$$

where, D denotes the crystallite size. The calculated dislocation density (δ) for Co_3O_4-006, Co_3O_4-007, Co_3O_4-008 and Co_3O_4-009 was 14.54×10^{-13} nm^{-2},14.23×10^{-13} nm^{-2},11.22×10^{-13} nm^{-2} and 10.94×10^{-13} nm^{-2}respectively [30].

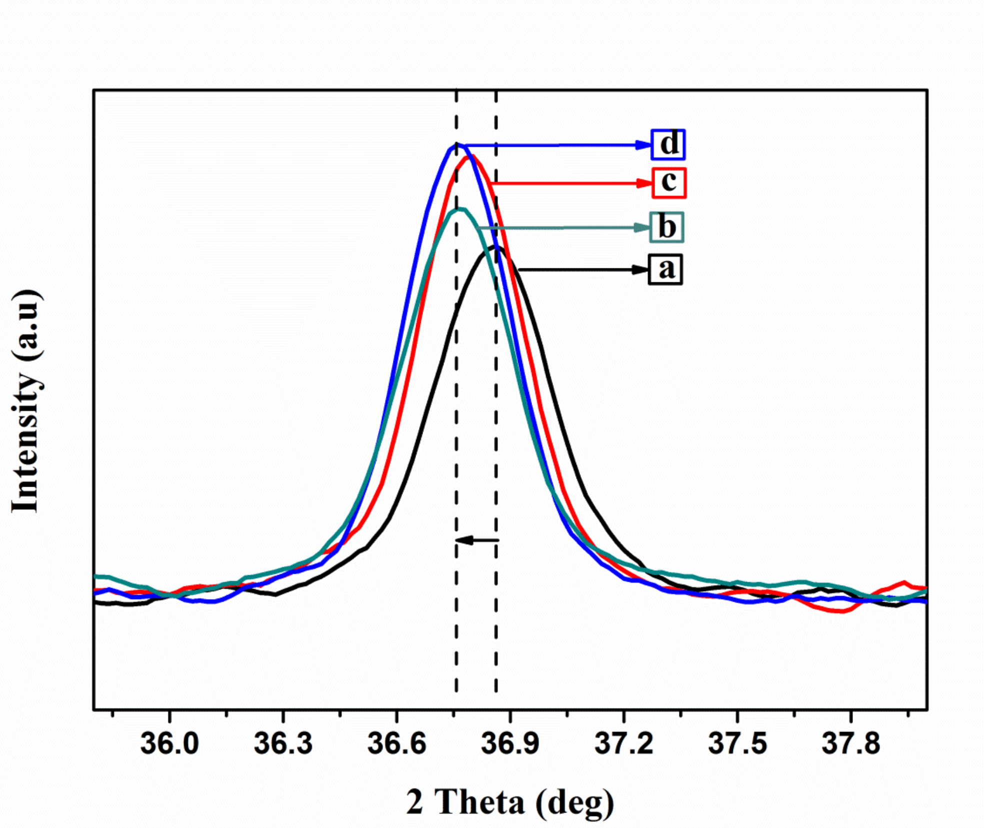

Figure 2. XRD pattern (311) intensity peak of a). Co_3O_4-006, b). Co_3O_4-007, c). Co_3O_4-008 and d). Co_3O_4-009

The calculated dislocation density of the prepared material linearly decreased. This may be due to the presence of surface charge properties [31]. The strain induced in nanoparticles was estimated from Williamson-Hall (W–H) method (5)

$$\varepsilon = \frac{\beta}{4\tan\theta} \quad \cdots\cdots\cdots\cdots\blacktriangleright \quad (5)$$

According to Hooke's law, stress (σ = Cε) can be calculated from the obtained strain. Where, C=1.46 ± 10^{10} N/m^2 is the bulk Young's modulus [30]. The calculated strain (ε) and stress (σ) of

Co_3O_4-006, Co_3O_4-007, Co_3O_4-008 and Co_3O_4-009 were found to be 0.3563, 0.3694, 0.3752, 0.3694 and 520, 539, 547, 580 MPa respectively. Figure 2 shows the high intensity (311) peak of Co_3O_4 nanoparticles. The peak of Co_3O_4-006 showed a peak shift towards lower angle side compared to Co_3O_4-007, Co_3O_4-008 and Co_3O_4-009 nanoparticles which may be due to the structural crystal defects that occur due to the change in the cobalt acetate concentration.

3.2 Fourier Transform Infrared Spectroscopy (FTIR) studies

Figure 3. represents the FTIR spectra of Co_3O_4 nanoparticles prepared from different Co(OAC) concentrations. The two peaks observed at574 cm^{-1} and 666 cm^{-1} were attributed to the fingerprint stretching vibrations of (M-O) bonds of Co-O in Co_3O_4, which were in good agreement with the previously reported value [28].

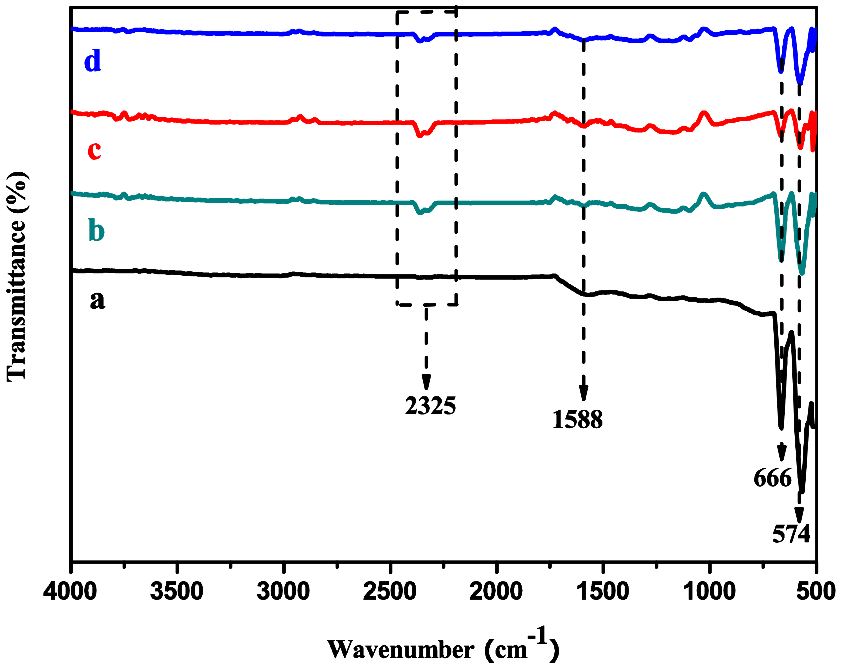

Figure 3. FTIR spectra of cobalt oxide nanoparticlesprepared from different concentration of cobalt acetate annealed at 450°C by sol-gel method (a) Co_3O_4-006, (b) Co_3O_4-007, (c) Co_3O_4-008 and (d) Co_3O_4-009

The band at 574 cm^{-1} corresponded to Co-O vibrations in octahedral sites of BOB_3 type, “B” represents CO^{3+} ions in the octahedral site and the band at 666 cm^{-1} corresponded to ABO_3 type, “A” represented the metal ions in the tetrahedral positions confirming the formation of spinel Co_3O_4 in pure phase [32]. The presence of some noises in the peaks may be due to the presence of polyvinyl pyrrolidone that was not completely combusted. The peak at 2325 cm^{-1} isascribedto the presence of CO_2 in the air medium [33]. A peak at 1588 cm^{-1} corresponded to the H-O-H bending vibration of the water molecules (or) alcohol present along with the prepared material [33, 34].

3.3 Raman spectroscopy studies

The Raman spectra of Co_3O_4-006, Co_3O_4-007, Co_3O_4-008 and Co_3O_4-009 are shown in the Figure 4. All the observed bands for Co_3O_4 were predicted by group theory for F3dm space group. The bands at 131 cm^{-1}, 502 cm^{-1} and 619 cm^{-1} were assigned to $3F_{2g}$ mode and702 cm^{-1} band at A_{1g} mode attributed to the octahedral and tetrahedral site in Co_3O_4 [3, 35]. The band at 469 cm^{-1} that wasoriginating from Eg mode, may be due to the surface defects created because of the surface oxidation of Co in Co_3O_4 [3].

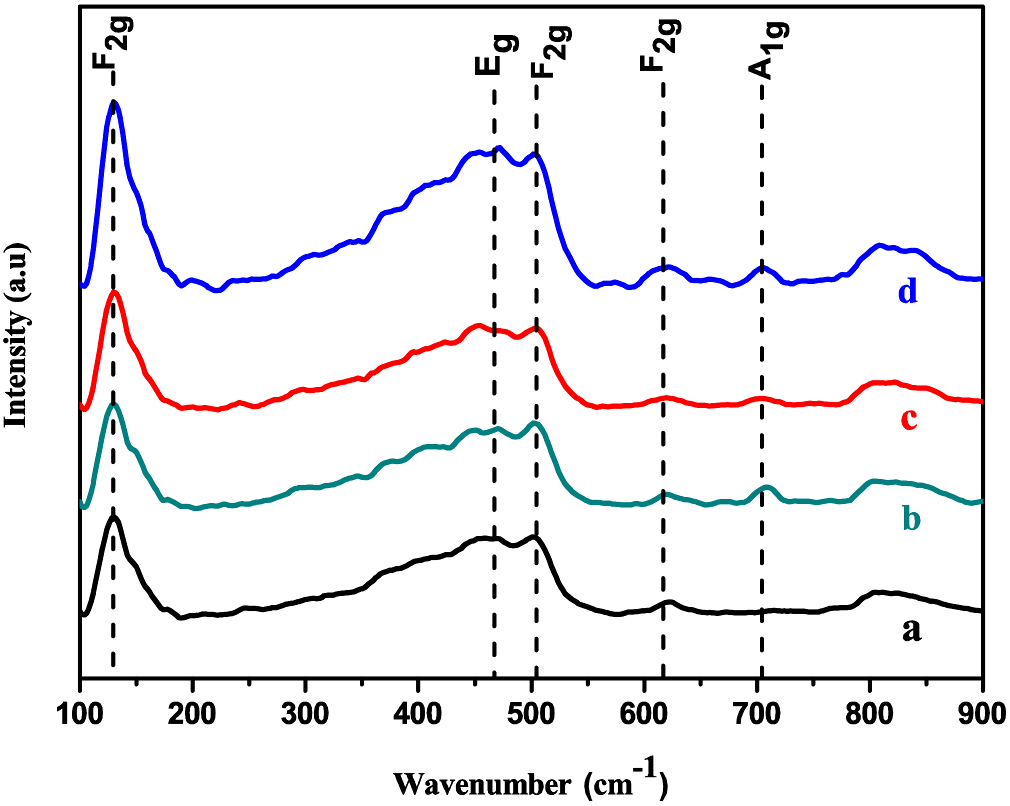

Figure 4. Raman spectrum of cobalt oxide nanoparticlesprepared at 450ºC by sol-gel method (a).Co_3O_4-006, (b).Co_3O_4-007, (c). Co_3O_4-008 and (d).Co_3O_4-009

3.4 Surface morphological studies

Figure 5. shows the different magnifications FE-SEM images of Co_3O_4-006, Co_3O_4-007, Co_3O_4-008 and Co_3O_4-009 nanoparticles. The morphology of the particles varied with varying concentration of cobalt acetate precursor. Nanospheres were observed with Co_3O_4-006 and Co_3O_4-007 (Fig. 5(a-f)). The size of the particle ranged from 50 to 100 nm. When the concentration increased to 0.08M the particle size of Co_3O_4-008 increased from nano to micro. The nanosphere particles agglomerate and bound together to form microspheres of size 1 µm. The increase in the size of the particle from nanometer to micrometer with respect to the change in the concentration of the Co(OAC) precursor clearly illustrates that the precursor quantity influences on the surface morphology of the formed product. The elemental composition of Co_3O_4 nanoparticles were clearly depicted in the

EDAX spectra (Figure 6). The sharp and intense peaks of Co and Oxygen (O) atoms confirmed the presence of Co_3O_4 nanoparticle without impurities. The TEM image of Co_3O_4-006 nanoparticles were presented in Figure 7(a-d). The particle size of around 50 nm coincides with the particle size observed from SEM analysis. The SAED pattern of HRTEM image showed the polymorphic rings which proved the high crystallinity of the sample as evidenced from XRD analysis.

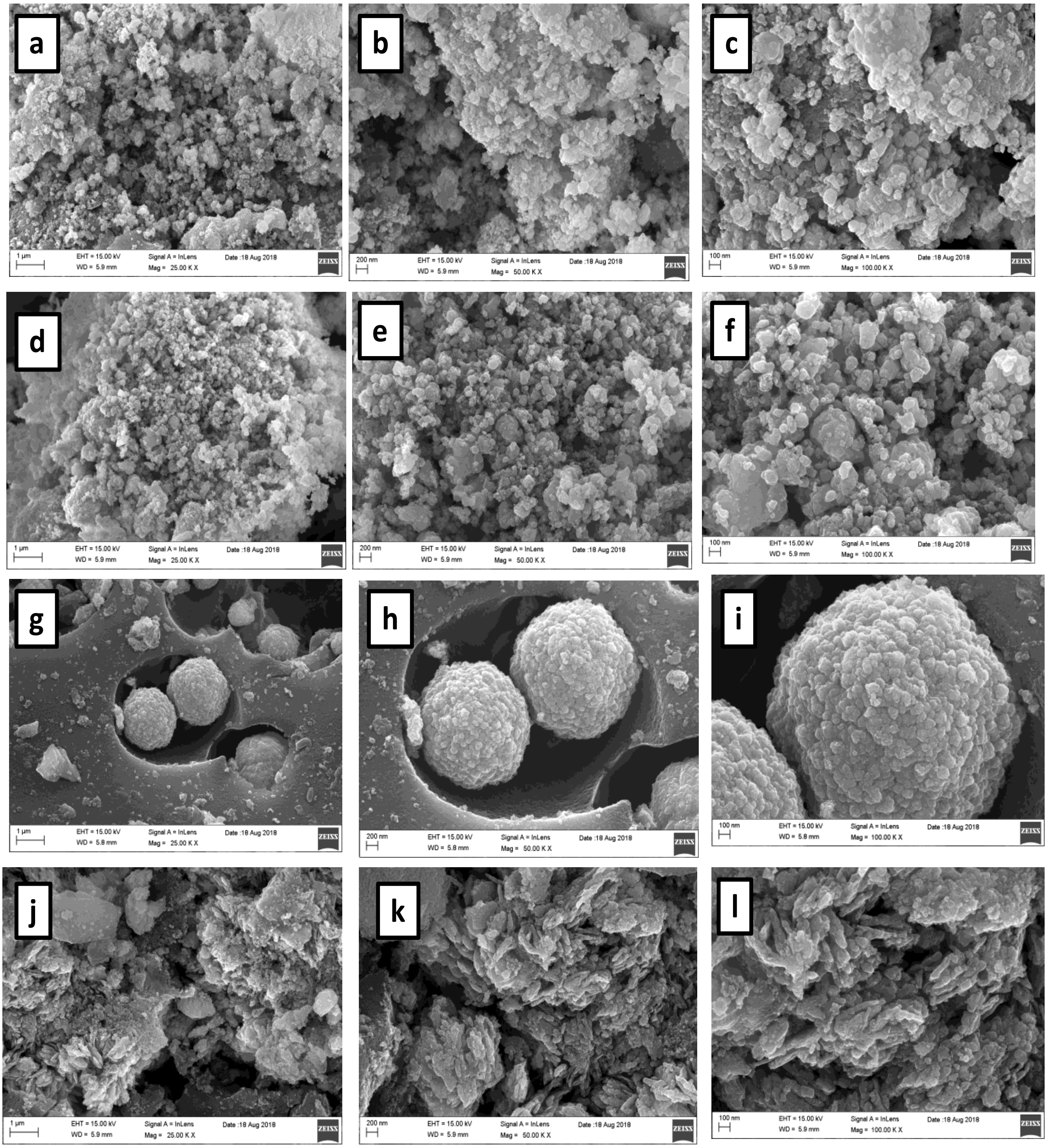

Figure 5. FE-SEM images of cobalt oxide nanoparticles prepared at 450ºC by sol-gel method (a-c). Co_3O_4-006,(d-f) Co_3O_4-007,(g-i) Co_3O_4-008and (j-l) Co_3O_4-009

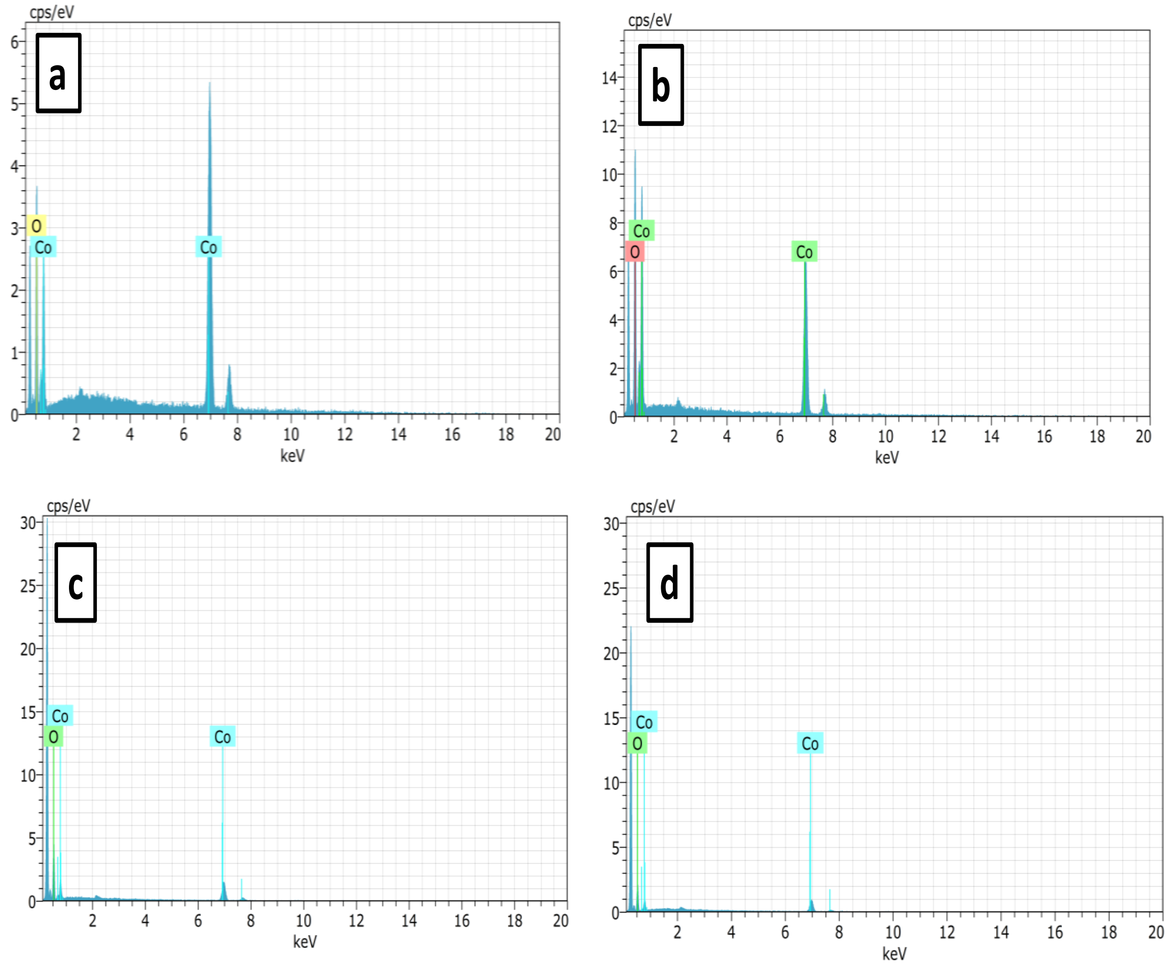

Figure 6. (a-d) EDAX spectra of cobalt oxide nanoparticlesprepared at 450ºC by sol-gel method at 450ºC (a).Co_3O_4-006, (b).Co_3O_4-007, (c). Co_3O_4-008 and (d).Co_3O_4-009

3.5 UV-Vis absorption studies

The optical property of the prepared Co_3O_4 nanoparticles were carried out by UV-Vis spectra and is presented in Figure 8. The optical properties of the synthesized materials deliver the impurity levels, energy band structure, localized defects, excitons, lattice vibrations and certain magnetic excitations [17]. The two broad absorbance peaks were observed between 500-600 nm and 800-850 nm respectively for all the Co_3O_4 nanoparticles, were in good agreement with the previous reports [28]. The direct energy band gap (E_g) of the synthesized samples was determined by using Tauc's relation (6).

$$(\alpha h\upsilon)^{n} = A^{*}(h\upsilon-E_{g}) \quad \cdots\cdots\cdots\cdots\rightarrow (6)$$

Where, α is the absorption coefficient, hυ is the photon energy and E_g is the band gap of the synthesized material, n- denotes the electronic transition (or) optical transition values 1/2, 2, 3/2 or 3 [28, 30]. If n=1/2, the transition is then the direct allowed transition, n=3/2 direct forbidden transition, n= 2 indirect allowed transition and if n=3 indirect forbidden transition. From the plots of $(\alpha h\upsilon)^2$ vs (hυ), direct band gap was found to be 1.29 eV and 3.34 eV for Co_3O_4-006, 1.39 eV and 3.53 eV for

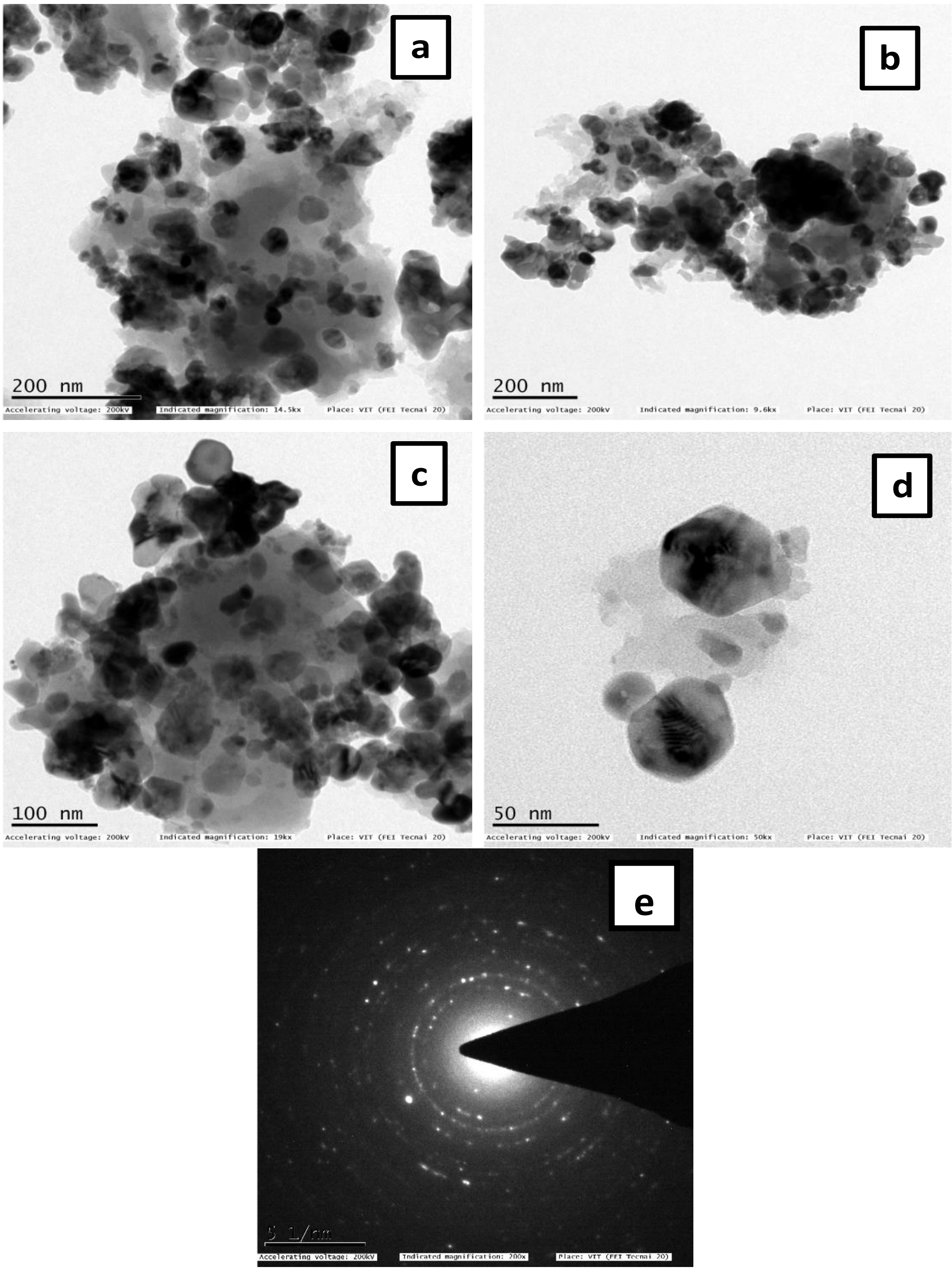

Figure 7. (a-d) HRTEM image and (e) SAED pattern of Co_3O_4-006 nanoparticles prepared at 450ºC by sol-gel method

Co_3O_4-007, 1.59 eV and 3.58 eV for Co_3O_4-008 and 1.63 eV and 3.65 eV for Co_3O_4- 009 nanoparticle (Figure 9). The band gap of the synthesized material linearly increases with increase in the concentration of the Co(OAC), which may be due to the increase in the particle size with respect to the concentration.

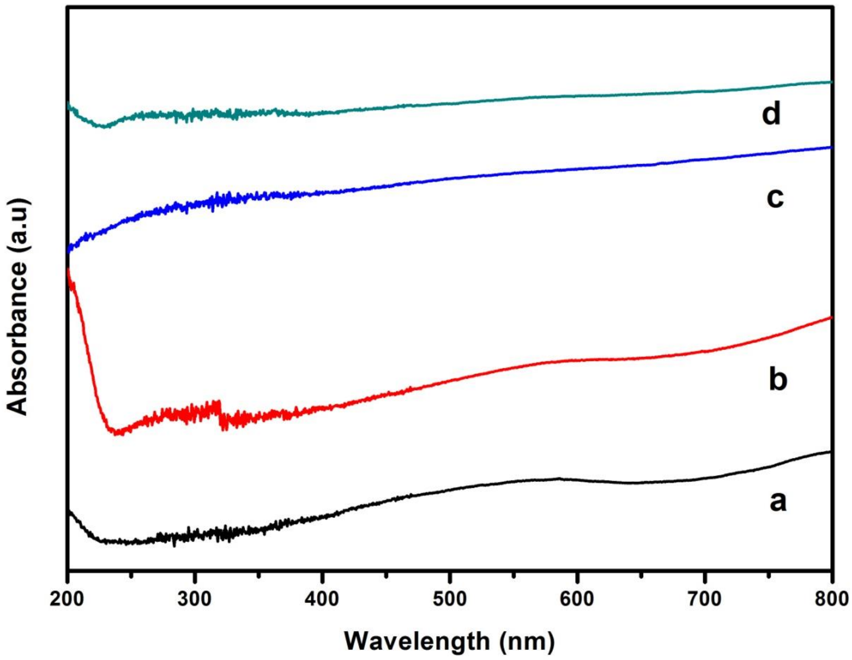

Figure 8. UV-Vis absorption spectra of cobalt oxide nanoparticlesprepared at 450ºC by sol-gel method (a).Co_3O_4-006, (b).Co_3O_4-007, (c). Co_3O_4-008 and (d).Co_3O_4-009

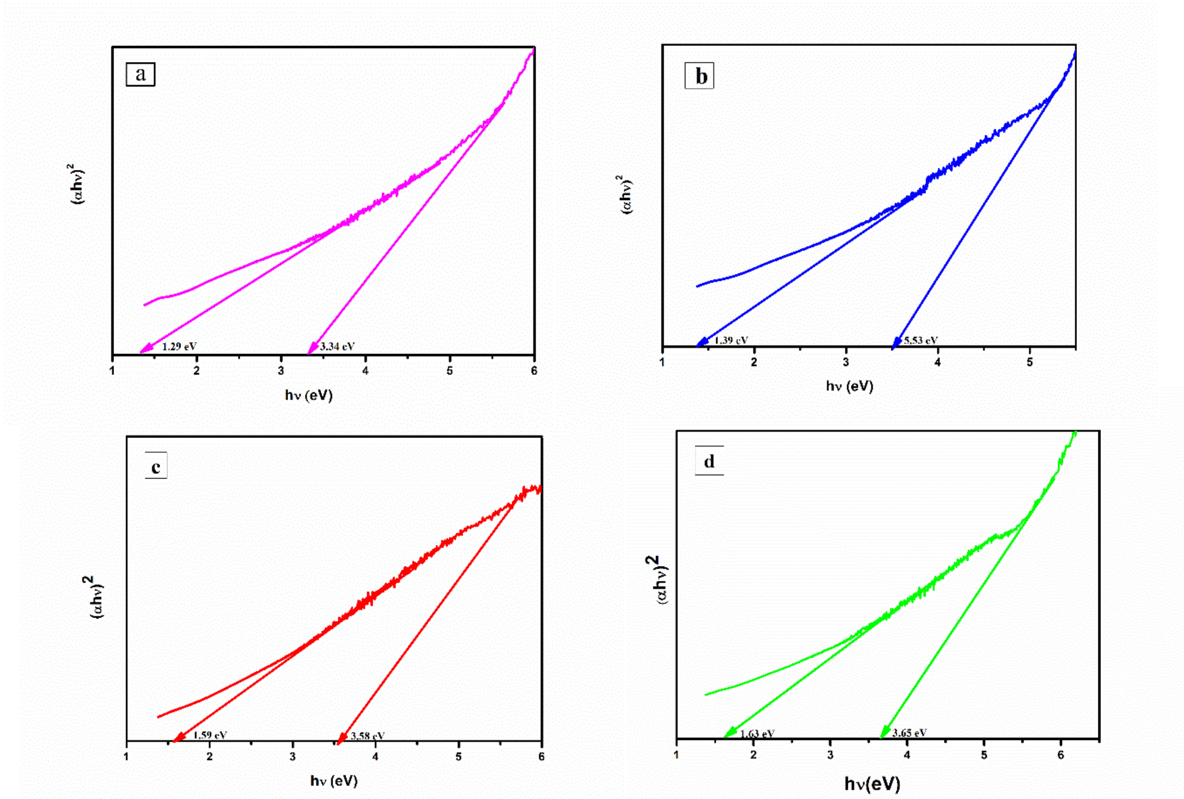

Figure 9. Band gap of cobalt oxide nanoparticlesprepared at 450ºC by sol-gel method (a).Co_3O_4-006, (b).Co_3O_4-007, (c). Co_3O_4-008 and (d).Co_3O_4-009

In addition, the quantum confinement effect may also be one of the reasons for linear increase in band gap energy [36]. Two different oxidation states persist in the cobalt (Co^{3+} and Co^{2+}) ion which may bethe reason for the existence of two absorption peaks in the UV-Vis spectroscopy. The charge transfer processes from O^{2-} to $Co^{2+}$and O^{2-} to Co^{3+} leads to the higher band gap and lower band gap energy respectively which was responsible for the existence of absorption bands.

3.6 Photoluminescence (PL) spectral analysis

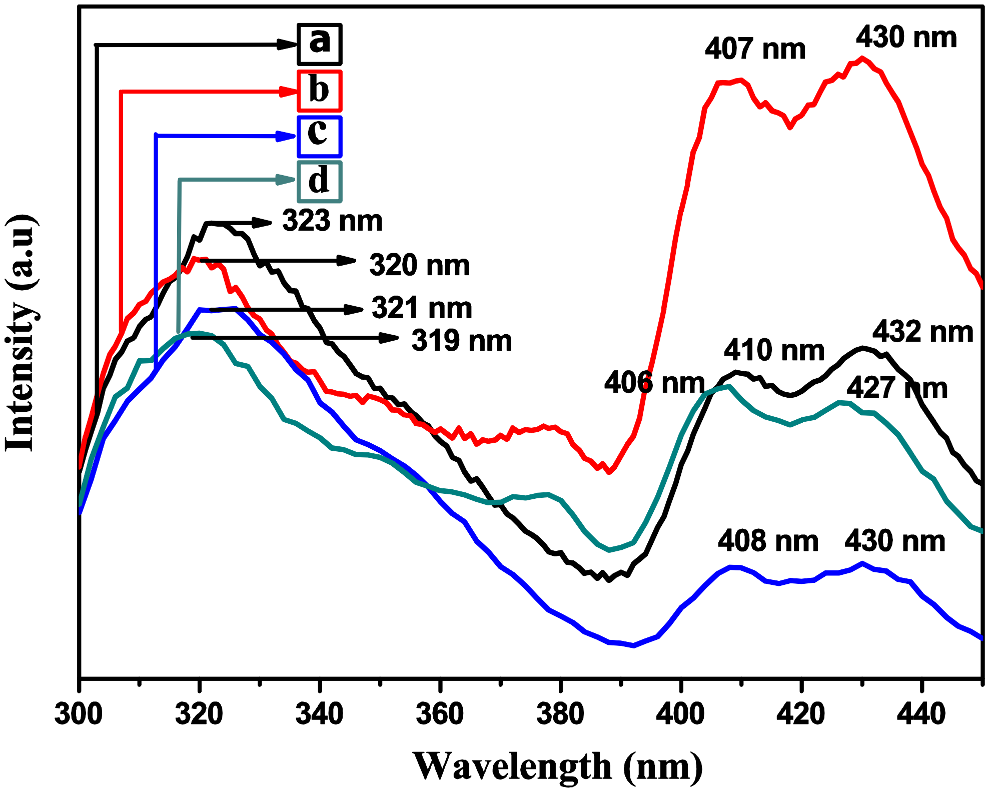

Figure 10. Photoluminescence spectra of cobalt oxide nanoparticlesprepared at 450°C by sol-gel method (a). Co_3O_4-006, (b). Co_3O_4-007, (c). Co_3O_4-008 and (d). Co_3O_4-009

Figure 10 corresponds to the PL spectra of Co_3O_4 nanoparticles prepared from four different concentrations. The Near Band Edge emission (NBE) (or) blue emission of the Co_3O_4 nanoparticles exhibited peaks at 323 nm, 321 nm, 320 nm and 319 nm and the peaks were observed at (410, 432), (407, 430), (408, 430), (406, 427) nm for Co_3O_4-006, Co_3O_4-007, Co_3O_4-008 and Co_3O_4-009 nanoparticles, respectively. The two bands observed near 400 nm for all the concentrations may be due to the oxygen vacancy created within the nanocrystalline particle that stabilized the cubic spinel structure of the Co_3O_4 nanoparticles. The change in the absorption and the emission properties and the moderate variation in the band gap of the nanoparticles may be due to presence of the impurities that induce the several occupied localized states leading to change in absorption and emission properties [37].

3.7 Photocatalytic activity of Co_3O_4 nanoparticles

The photocatalytic activity of Co_3O_4 nanoparticles were studied towards the degradation of methylene blue dye under visible light irradiation and presented in Figure 11. The decrease in the concentration of methylene blue dye after its reaction with the Co_3O_4photocatalyst under visible light was calculated by measuring the absorbance at regular time intervals.

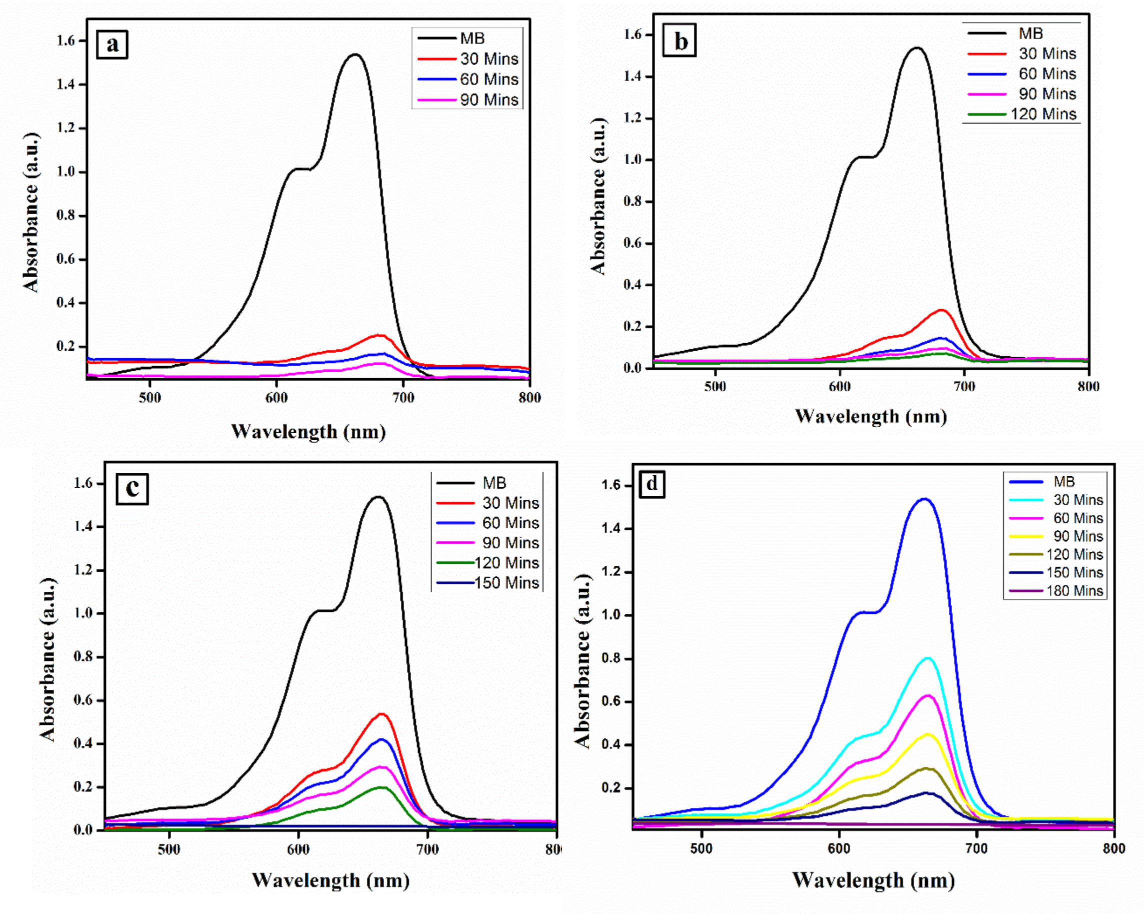

Figure 11. Photocatalytic degradation of methylene blue dye using cobalt oxide nanoparticles as photocatalyst(a). Co_3O_4-006, (b). Co_3O_4-007, (c). Co_3O_4-008 and (d). Co_3O_4-009

Observation revealed that there was a gradual reduction in the absorbance with increase in irradiation time. About 93.8% of methylene blue dye was degraded within 90 minutes with Co_3O_4-006 nanoparticles whereas for Co_3O_4-007, Co_3O_4-008 and Co_3O_4-009 nanoparticles the degradation of methylene blue were around 95, 98 and 97% (Fig. 12b) at 120, 150 and 180 minutes respectively. The methylene blue dye degradation ability when treated with the other metal oxide photocatalyst is shown in Table.1.The time taken for the degradation of methylene blue dye when treated with the other metal oxide photocatalyst is shown in table.1. When metal oxide like TiO_2 is used as the photocatalytic material for the degradation of methylene blue dye the degradation efficiency was just 48.2 % at 100 minutes whereas the same TiO_2 when used along with graphene oxide or silver the efficiency increased to 79.8% at 360 minutes (Table.1). When metal chalcogenides like MoS_2-FeZnO is used as a photocatalyst 95% degradation takes place at 140 minutes but compared to other photocatalyst Co_3O_4

pristine material is degrading 93% of the methylene blue dye within 90 minutes (Table.1). The table illustrates that the when the percentage of the degradation is high the time taken for the degradation is also comparatively high with other photocatalytic material, but with Co_3O_4 the degradation efficiency is very high at a short duration of 90 minutes.

Table 1. Response of methylene blue dye degradation with respect to different photo catalyst

Material	Degradation Capacity (%)	Time (min)	Reference
TiO_2 Nano tubes	48.2	100	38
Ag-TiO_2/GO nanocomposite	79.8	360	39
Mn-Layered Double Oxide	91.5	60	40
CoMnFe-Layered Double oxide	92	60	41
ZnO/GO	86.9	103	42
$Rb_{0.27}WO_3$/NiFe-Calcined Layered Double Hydroxides	91	210	43
BiS_3/ZnO	91.5	200	44
MoS_2-FeZnO	95	140	45
$CoFe_2O_4$	80	140	46
Co_3O_4	93.8	90	This Work

3.8 Photocatalytic kinetics

The kinetics of the methylene blue degradation using Co_3O_4photocatalysts were calculated under optimized parameter conditions: photocatalyst dose: 0.1 g, methylene blue concentration: 10 mg/L. A graph of $\ln(C_t/C_o)$ against time (min) was drawn and is presented in Figure 13. The rate of the order of the reaction is inferred from the kinetic study. The graph illustrates a straight line with a positive slope and the rate constant of 0.0186 min^{-1}, 0.0152 min^{-1}, 0.0126 min^{-1} and 0.0077 min^{-1} for Co_3O_4-006, Co_3O_4-007, Co_3O_4-008 and Co_3O_4-009 respectively. The positive slope indicates that the reaction is biomolecular following the second order reaction. From the graph, the correlation coefficient (R^2) and the reaction rate constants were calculated. The R^2 value of Co_3O_4-006 was found to be 0.9585 nearer to 1 when compared to the R^2 values of Co_3O_4-007, Co_3O_4-008 and Co_3O_4-009 which was 0.9268, 0.9246 and 0.6228respectively.Co_3O_4-006 with higher R2 showed the faster rate of degradation compared to Co_3O_4-007, Co_3O_4-008 and Co_3O_4-009 nanoparticles. The photodegradation mechanism took place when the photocatalyst were irradiated with light energy equal (or) higher than that of material band gap.

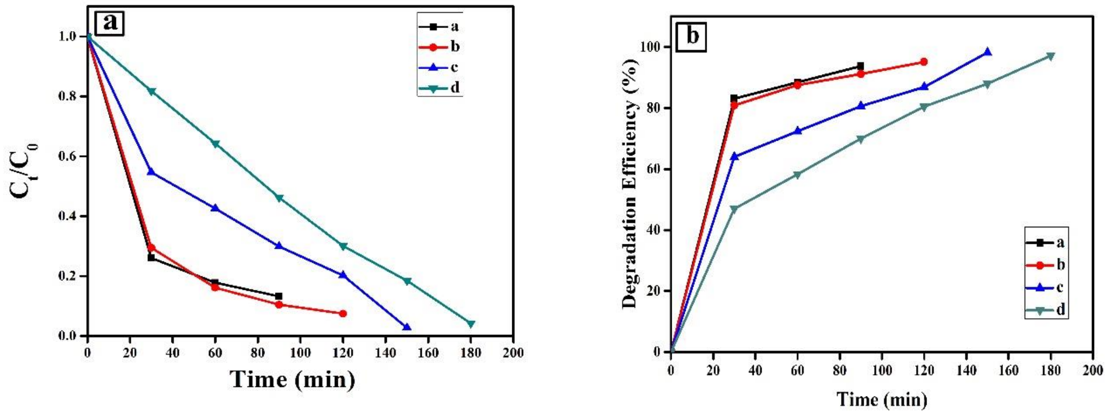

Figure 12. (a) Change in dye concentration with respect to time and (b) Percentage of methylene blue dye degradation with respect to time. (a). Co_3O_4-006, (b). Co_3O_4-007, (c). Co_3O_4-008 and (d). Co_3O_4-009

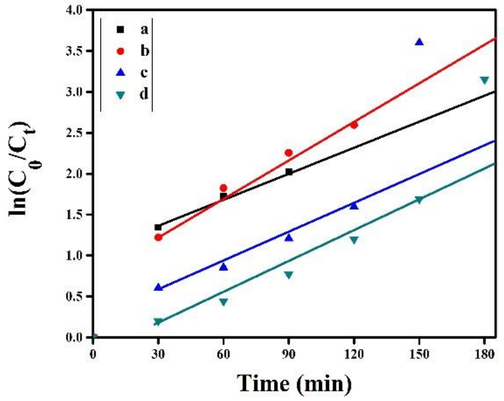

Figure 13. Kinetic plot for photodegradation of methylene blue dye of (a). Co_3O_4-006, (b). Co_3O_4-007, (c). Co_3O_4-008 and (d). Co_3O_4-009

While irradiation, electrons and holes are separated in the valence band and the electrons are excited to the conduction band [47, 48]. Ozone and H_2O_2 acts as the sacrificial oxygen donors in the degradation process of photo-fentonsreaction [49-52]. In the present study air acted as the potential oxidizing agent to perform photodegradation process instead of the conventional sacrificial oxygen donors.

$$Co_3O_4 + h\upsilon \rightarrow h^+ + e^- \quad \cdots\cdots\cdots\cdots\rightarrow (7)$$

$$H_2O + h^+ \rightarrow H^+ + OH^\bullet \quad \cdots\cdots\cdots\cdots\rightarrow (8)$$

$$O_2 + e^- \rightarrow {}^\bullet O^{2-} \quad \cdots\cdots\cdots\cdots\rightarrow (9)$$

$$\text{Organic dye (OD)} + (OH^\bullet / {}^\bullet O^{2-}) \rightarrow \text{degradation} \quad (10)$$

$$OD + h\upsilon \rightarrow OD^* \cdots\cdots\cdots\cdots\cdots\cdots\rightarrow (11)$$

$$OD^* + Co_3O_4 \rightarrow Co_3O_4(e) \cdots\cdots\cdots\cdots\cdots\cdots\rightarrow (12)$$

$$Co_3O_4(e) + O_2 \rightarrow {}^{\bullet}O^{2-} + Co_3O_4 \cdots\cdots\cdots\cdots\cdots\cdots\rightarrow (13)$$

The Co_3O_4 nanoparticles on irradiation with hυ formed the active species such as super hydroxy and superoxy radical (eqn. 8 & 9) which were responsible for effective photodegradation of organic dye that reacted vigorously in the degradation process. On illumination of photons the methylene blue dye created reactive species (eqn 11 to 13) inserted electron back into the lattice plane of Co_3O_4 which helped in the formation of superoxy radical in the presence of available oxygen in the system that further enhancedthe photodegradationprocess [46].

4. CONCLUSION

Spinel cubic structured Co_3O_4 nanoparticles were prepared from cobalt acetate precursor using polymer assisted sol-gel method. The XRD patterns confirmed the presence of octahedral and tetrahedral sites of Co_3O_4 with crystallite size of 26.22 nm, 26.50 nm, 29.85 nm and 30.23 nm. The FTIR study confirmed Co_3O_4 formation with the presence of strong M-O peaks at 571 cm^{-1} and 662 cm^{-1}. The particle size ranged from 50 nm to 1 µm with respect to the change in precursor concentration. The optical band gap varied from 1.29 eV and 3.34 eV for Co_3O_4-006, 1.39 eV and 3.53 eV for Co_3O_4-007, 1.59 eV and 3.58 eV for Co_3O_4-008 and 1.63 eV and 3.65 eV for Co_3O_4-009 nanoparticles. The photocatalytic degradation activity was 93.8% for Co_3O_4-006 nanoparticles at 90 minutes compared to Co_3O_4-007, Co_3O_4-008 and Co_3O_4-009 undergoes 90, 86 and 82% at 120, 150 and 180 minutes respectively. The change in the quantity of the cobalt acetate precursor influenced the surface morphology and particle size. The particle size increased from nanodimensions to microdimensions with change in concentration whereas the dye degradation took place in all the cobalt oxide particles irrespective to the precursor concentration but the time taken for the degradation was influenced by the precursor concentration. The degradation was fast with Co_3O_4-006 nanoparticles than the other concentrations.

References

1. X. Lou, J. Han, W. Chu, X. Wang and Q. Cheng,*Mater. Sci. Eng. B.*, 137 (2007) 268.
2. D. Zhang, L. Ren, X. Hao, B. Pan, M. Wang, J. Ma, F. Li, S. Li and Z. Tong, *Appl. Surf. Sci.*, 355 (2015) 547.
3. R. Edla, N. Patel, M. Orlandi, N. Bazzanella, V. Bello, C. Maurizio, G. Mattei, P. Mazzoldi and A. Miotello, *Appl. Catal. B.*, 166 (2015) 475.
4. T. Robinson, G. McMullan, R. Marchant and P. Nigam, *Bioresour. Technol.*, 77 (2001) 247.
5. D. Georgiou, P. Melidis, A. Aivasidis and K. Gimouhopoulos, *Dyes. Pigm.*, 52 (2002) 69.
6. P.P. Zamora, A. Kunz, S.G. Moraes, R. Pelegrini, P.C. Moleiro, J. Reyes and N. Duran, *Chemosphere.*, 1999 (38) 835.
7. M. Ghosh, E.V. Sampathkumaran and C.N.R. Rao, *Chem. Mater.*, 17 (2005) 2348.
8. A.M. Cao, J.S. Hu, H.P. Liang, W.G. Song, L.J. Wan, X.L. He, X.G. Gao and S.H. Xia, *J. Phys. Chem. B.*, 110 (2006) 15858.

9. K.I. Choi, H.R. Kim, K.M. Kim, D.W. Li, G.Z. Cao and J.H. Lee, *Sensor. Actuat. B-Chem,*146 (2010) 183.
10. W.Y. Li, L.N. Xu and J. Chen, *Adv. Funct. Mater.,* 15 (2005) 851.
11. F. Manteghi, S.H. Kazemi, M. Peyvandipoor and A. Asghari, *RSC.Adv.,* 5 (2015) 76458.
12. D. Barreca, M.C. Yusta, A. Gasparotto, C. Maccato, J. Morales, A. Pozza, C. Sada, L. Sanchez, E. Tondello, *J. Phys. Chem C.,* 114 (2010) 10054.
13. B. Guo, C.S. Li, Z.Y. Yuan, *J. Phys. Chem.C.,* 114 (2010) 12805.
14. P. Poizot, S. Laruelle, S. Grugeon, L. Dupont and J.M. Tarascon, *Nat.,* 407 (2000) 496.
15. W.L. Yao, J. Yang, J.L. Wang and Y. Nuli, *J. Electrochem. Soc.,* 155 (2008) 903.
16. L.H. Hu, Q. Peng and Y.D. Li, *J. Am. Chem. soc.,* 130 (2008) 16136.
17. L.H. Hu, K.Q. Sun, Q. Peng, B.Q. Xu and Y.D. Li, *Nano Res.,* 3 (2010) 363.
18. X.W. Xie, Y. Li, Z.Q. Liu, M. Haruta and W.J. Shen, *Nat.,* 458 (2009) 746.
19. J. Ryu, S.W. Kim, K. Kang and C.B. Park, *ACS Nano,* 4 (2010) 159.
20. S.G. Kandalkar, C.D. Lokhande, R.S. Mane and S.H. Han, *Appl. Surf. Sci.,* 253 (2007) 3952.
21. X. Zhao, Z. Pang, M. Wu, X. Liu, H. Zhang, Y. Ma, Z. Sun, L. Zhang and X. Chen,*Mater. Res. Bull.,* 48 (2013) 92.
22. T. Warang, N. Patel, A. Santini, N. Bazzanella, A. Kale and A. Miotello, *Appl. Catal. A.,* 423 (2012) 21.
23. Y. Chen, L. Hu, M. Wang, Y. Min and Y. Zhang, *Colloid. Surf. A: Physicochem. Eng. Asp.,* 336 (2009) 64.
24. S. Mallakpour, E. Khadem, *Green. Polym. Compos. Techn: Properties and Applications,* (2016) 261.
25. S. Mallakpour, V. Behranvand, *Colloid. Polym. Sci.,* 292 (2014) 2275.
26. S. Mallakpour, E. Khadem, *J. Polym. Res.,* 24 (2017) 86.
27. S. Mallakpour, N. Nouruzi, *J.Polym.,* 89 (2016) 94-101.
28. S.N. Karthick, K.V. Hemalatha, C. Justin Raj, H.J. Kim and M. Yi, *J. Nanopart. Res.,* 15 (2013) 1474.
29. W.N.W. Ismail, *J. Sol-Gel Sci. Techn.,*78 (2016) 698.
30. N. Senthilkumar, E. Vivek, M. Shankar, M. Meena, M. Vimalan and I.V. Potheher, *J. Mater. Sci-Mater. El.,* 29 (2018) 2927.
31. N. Senthilkumar, M. Ganapathy, A. Arulraj, M. Meena, M. Vimalan and I. VethaPotheher, *J. Alloys. Compd.,*750 (2018) 171.
32. M. Pudukudy, Z. Yaakob, *Chem. Pap.,* 68 (2014) 1087.
33. R. Jeyachitra, V. Senthilnathan and T.S. Senthil,*J. Mater. Sci-Mater. El.,*29 (2018) 1189.
34. Arulraj, S. Bhuvaneshwari, G. Senguttuvan and M. Ramesh, *J. inorg. Organomet. Polym.mater.,*28 (2018) 1029.
35. R. Edla, N. Patel, Z.E. Koura, R. Fernandes, N. Bazzanella and A. Miotello, *Appl. Surf. Sci.,* 302 (2014)105.
36. K. Agilandeswari, A. Rubankumar, *Synth. React. Inorg. M.,* 46 (2016) 502.
37. S. Gopinath, K. Sivakumar, B. Karthikeyen, C. Ragupathi and R. Sundaram, *Physica. E low. Dimens. Syst. nanostruct.,*81 (2016) 66.
38. Chien, Wei, Chi-Yu Lin, Shang-Te Tsai, Cheng-Fu Yang, Chiu-Chen Chang, and Shih-Tung Shu. *Sensors and Materials*, (2018), 655.
39. Choi, Bo-Kyung, Woong-Ki Choi, Soo-Jin Park, and Min-Kang Seo. *Journal of Nanoscience and Nanotechnology,* 18, no. 9 (2018) 6075–80.
40. Dou, Ruyan, Jianfeng Ma, Daiqin Huang, Changhai Fan, Wenchang Zhao, Mingguo Peng, and Sridhar Komarneni. *Applied Clay Science,* 161 (2018) 235–41.
41. Huang, Daiqin, Jianfeng Ma, Changhai Fan, Kai Wang, Wenchang Zhao, Mingguo Peng, and Sridhar Komarneni. *Applied Clay Science,* 152 (2018) 230–38.

42. Zarrabi, Mahdi, Mohammad Haghighi, and Reza Alizadeh. *UltrasonicsSonochemistry*, 48 (2018) 370–82.
43. Zhao, Guoqing, Dan Zhang, Yaliang Huang, Jingang Yu, Xinyu Jiang, and FeipengJiao*Advanced Powder Technology*, 10 (2018) 2491–2500.
44. Velanganni, S., A. Manikandan, J. Joseph Prince, C. Neela Mohan, and R. Thiruneelakandan. *Physica B: Condensed Matter* 545 (2018) 383–89.
45. Ghalajkhani, Ali, Mohammad Haghighi, and Maryam Shabani. *Journal of Photochemistry and Photobiology A: Chemistry* 359 (2018) 145–56..
46. Kalam, Abul, Abdullah G. Al-Sehemi, Mohammed Assiri, Gaohui Du, Tokeer Ahmad, Irfan Ahmad, and M. Pannipara. *Results in Physics*, 8 (2018) 1046–53.
47. U.G. Akpan, B.H. Hameed, *J. Hazard. Mater.*, 170 (2009) 520.
48. K. Kocl, L. Obalova and Z. Lacny, *Chem. Pap.*, 62 (2008) 1.
49. Q. Xiao, J. Zhang, C. Xiao and X. Tan, *Catal. Commun.*,9 (2008)1247.
50. J.H. Ramirez, M.A. Vicente and L.M. Madeira, *Appl. Catal. B-Environ.*, 98 (2010) 10.
51. G. Li, X.S. Zhao and M.B. Ray, *Sep. Purif. Technol.*, 55 (2007) 91.
52. G.S. Wang, S.T. Hsieh and C.S. Hong, *Water Res.*, 34 (2000) 3882.